
PERGAMON

Journal of Quantitative Spectroscopy & Radiative Transfer 70 (2001) 261–272

Journal of Quantitative Spectroscopy & Radiative Transfer

www.elsevier.com/locate/jqsrt

Scattering cross sections of randomly oriented coated spheroids

A. Quirantes*, A.V. Delgado

Departamento de Física Aplicada, Facultad de Ciencias, Universidad de Granada, 18071 Granada, Spain

Received 27 May 1998; accepted 24 August 1998

Abstract

The extended boundary condition method (EBCM), or T-matrix method, has been applied to the determination of scattering cross sections of coated spheroidal particles in random orientation. We report the effects of varying size and core/shell ratio for a number of axial ratios. Different scattering properties of equal-volume prolate and oblate spheroids, as well as the effect of nonsphericity on thin-shell-coated systems are considered. We discuss some convergence strategies for coated-particle EBCM calculations. © 2001 Elsevier Science Ltd. All rights reserved.

Keywords: EBCM; Nonspherical coated particles

1. Introduction

Waterman's T-matrix method [1–3] is one of the most widely used method for calculating electromagnetic scattering properties of nonspherical particles. It is specially suitable for axisymmetric homogeneous particles [4] and can be efficiently applied to ensembles of randomly oriented particle systems [5,6]. T-matrix calculations of multilayered systems would also allow the study of coated particles beyond the usual Aden–Kerker formulation for coated spheres [7,8].

The T-matrix formulation was generalized by Peterson and Ström [9,10] for multilayered dielectric objects. But, while calculations have been done for nonspherical particles [11,12], little attention seems to have been paid to the case of random orientation (an exception can be found e.g. in Wang et al. [13]). We can think of two reasons for this. One is that many applications do not demand orientational averaging, so the T-matrix approach becomes less attractive when compared

* Corresponding author.
E-mail address: aquiran@ugr.es (A. Quirantes).

0022-4073/01/$ - see front matter
PII: S0022-4073(00)00136-9

to fixed-orientation methods such as separation of variables [14] or the generalized point-matching technique [15,16]. The other is that the ill-conditioning of T-matrix calculations for extreme cases [17] (large sizes, absorbing materials, high nonsphericity) can make it so unstable in coated particle systems that it might seem worthwhile to resort to more time-consuming methods combining both calculations at fixed orientations and standard angle integration, thereby gaining accuracy at the expense of computer time and complexity.

In the present paper we show that the T-matrix can be applied to coated spheroidal particles in random orientation for a range of sizes, eccentricities and core/shell ratios. An adequate implementation of convergence procedures can allow us to take advantage of the full EBCM potential with no sacrifice whatsoever in accuracy. Finally, as it is our feeling that such calculations should be enabled to be made on medium- and small-size computers, a Fortran computer code has been developed that runs in PC desktop computers (486, Pentium), although it can also be compiled and run on larger, Unix-based mainframe machines.

2. Theory

In Waterman's T-matrix approach [1], both the incident and the scattered time-independent electric fields $\mathbf{E}_{\mathrm{inc}}(r)$, $\mathbf{E}_{\mathrm{sca}}(r)$ are expanded in vector spherical harmonics [18] $\mathbf{M}_{mn}$, $\mathbf{N}_{mn}$:

$$E_{\mathrm{inc}}(r) = \sum_{n=1}^{\infty} \sum_{m=-n}^{n} [a_{mn} Rg\mathbf{M}_{mn}(kr) + b_{mn} Rg\mathbf{N}_{mn}(kr)]. \tag{1}$$

$$E_{\mathrm{sca}}(r) = \sum_{n=1}^{\infty} \sum_{m=-n}^{n} [p_{mn}\mathbf{M}_{mn}(kr) + q_{mn}\mathbf{N}_{mn}(kr)]. \tag{2}$$

The linearity of Maxwell's equations enables us to relate the scattered (p_{mn}, q_{mn}) and incident (a_{mn}, b_{mn}) field coefficients by means of a transition (T) matrix:

$$p_{mn} = \sum_{n'=1}^{\infty} \sum_{m'=-n'}^{n'} [T^{11}_{mnm'n'} a_{m'n'} + T^{12}_{mnm'n'} b_{m'n'}], \tag{3}$$

$$q_{mn} = \sum_{n'=1}^{\infty} \sum_{m'=-n'}^{n'} [T^{21}_{mnm'n'} a_{m'n'} + T^{22}_{mnm'n'} b_{m'n'}]. \tag{4}$$

The T matrix elements depend on the particle (size, shape, composition, orientation) but not on the nature of the incident and scattered fields, so they need to be calculated only once and then averaged for all directions of incidence and scattering, which equals to averaging on particle orientation. It is usually calculated for the so-called natural reference frame of the particle, and can be written in compact notation as

$$\mathbf{T} = -\mathbf{B} * \mathbf{A}^{-1} = \begin{pmatrix} T^{11} & T^{12} \\ T^{21} & T^{22} \end{pmatrix}. \tag{5}$$

For a two-layered axisymmetric object (characterized by refractive indices m_1 for core and m_2 for shell), the T matrix is given by [9]

$$\mathbf{T} = -[\mathbf{B}_2 + \mathbf{BB}_2 * \mathbf{T}_1] * [\mathbf{A}_2 + \mathbf{AA}_2 * \mathbf{T}_1]^{-1}, \tag{6}$$

where $\mathbf{T}_1$ is the transition matrix for the inner layer, as derived in the homogeneous case [9,13], with relative refractive indices m_1/m_2, (inner), 1 (outer) and incident radiation wavenumber $k_o m_2$. The matrices $\mathbf{B}_2$, $\mathbf{A}_2$ are such that $-\mathbf{B}_2 * (\mathbf{A}_2)^{-1}$ is the T-matrix for the outer layer, with inner and outer indices $(m_2, 1)$. Finally, the matrix $\mathbf{BB}_2$ is the same as $\mathbf{B}_2$, except that the Bessel functions of the first kind with argument kr are replaced by Hankel functions with the same argument; the same applies to the $\mathbf{AA}_2$ and $\mathbf{A}_2$ matrices.

Once the T matrix is calculated for the particle in its natural reference frame (with the z-axis along the axis of symmetry), cross sections can be computed. For an axisymmetric particle, the T matrix divides itself into m smaller, independent submatrices. The expressions for extinction and scattering cross sections are [5]

$$C_{\text{ext}} = \frac{2\pi}{k^2} \text{Re} \sum_{n=1}^{\infty} \sum_{m=-n}^{n} (T_{mnn}^{11} + T_{mnn}^{22}). \tag{7}$$

$$C_{\text{sca}} = \frac{2\pi}{k^2} \sum_{i,j=1}^{2} \sum_{n=1}^{\infty} \sum_{n'=1}^{\infty} \sum_{m=0}^{\text{Min}(n,n')} (2 - \delta_{m0}) |T_{mnn'}^{ij}|^2. \tag{8}$$

2.1. Convergence considerations

In practical T-matrix computations, the series expansion for the incident and scattered fields (Eqs. (1) and (2)) are truncated after a finite number of terms. Enough terms must be included so that the solution (cross sections, in our case) will converge within the desired accuracy; on the other hand, an excessive number of terms could result in a waste of computing time, as well as possible instabilities in the matrix calculation process and a loss of accuracy.

Following Mishchenko's criterion [6], the number of terms $n_{\max}$ is found by calculating the values of C_1 ($= C_{\text{ext}}$, $m = 0$) and C_2 ($= C_{\text{sca}}$, $m = 0$) until the relative differences of $C_1(n_{\max})$ and $C_1(n_{\max} - 1)$ are less than a given accuracy value Δ (same procedure for C_2). Our first guess is $n_{\max} = n_s$, where n_s is given by Wiscombe's rule [19] for spheres ($n_s = x + 4x^{1/3} + 2$) using as value of x the equivalent-volume-sphere size parameter kr_{eq}.

However, the existence of two boundaries (core–shell and shell–medium) suggests the calculation of two sets of matrices, and therefore, two values of $n_{\max}$. By using, for example, a single matrix size where the core size is a small fraction of the total particle, we risk taking either too many terms for the core (and possible diverging results) or too few terms for the shell (and lose accuracy). And, while forcing the use of a single matrix size can be acceptable in some cases, it will yield erroneous results in others.

A solution we propose is to check the matrix size requirements for both the inner boundary (matrix $\mathbf{T}_1$ in Eq. (6)) and the outer boundary (matrices $\mathbf{A}_2$, $\mathbf{B}_2$, $\mathbf{AA}_2$, $\mathbf{BB}_2$), thus resulting in two $n_{\max}$ parameters: n_{mc}, n_{ms} for core and shell expansions, respectively. A similar criterion is used for light scattering calculations of coated spherical particles [8,20]. In accordance with it, we

furthermore demand that $n_{ms} > n_{mc}$; Eq. (6) can be calculated by making $(\mathbf{T}_1)_{nn'} = 0$ for $\mathrm{Max}(n, n') > n_{mc}$.

The convergence in N_g (the number of Gauss quadrature points for the calculation of matrix elements) is also calculated for both core and shell. During the process of determining n_{mc}, a number $N_{gc} = 4n_{mc}$ is fixed. After n_{mc} has been determined, N_{gc} is increased in steps of four until the extinction and scattering cross sections for $\mathbf{T}_1$ (assuming no outer layer exists) converges to the desired accuracy Δ. The same process is carried out for n_{ms}, thus yielding a N_{gs} value for the outer boundary matrices. As a rule of thumb, we have found $N_g = 4n_m$ to be a good value in all but the most demanding cases (high nonsphericity values, for instance).

3. Results and discussion

In this section we show and compare results on the extinction efficiencies for particles with refractive indices 2.32 for core, 1.2 for shell and 1 for medium. This choice closely corresponds to particles with a hematite core and an yttrium basic carbonate coating, for a vacuum wavelength $\lambda_o = 488$ nm [21,22], except that the imaginary part of hematite refractive index is disregarded. This is done in order to outline the effects of size/shape on cross efficiency curves, which are generally smoother for highly absorbing particles. The accuracy parameter Δ is taken as 10^{-4}. Extinction efficiencies are defined as

$$Q_{ext} = \frac{C_{ext}}{G}, \qquad Q_{sca} = \frac{C_{sca}}{G} \tag{9}$$

(for nonabsorbing particles, $C_{ext} = C_{sca}$), where G is a relevant surface parameter of the particle. We have used $G = \pi r_{eq}^2$, where r_{eq} is the radius of the equal-volume sphere. Other definitions, such as the projected cross section of the particles in the ensemble [23,24], can also be used.

The following convention is used. kr_{eq} is the dimensionless equal-volume-sphere size parameter; q is the core/shell size ratio; ε is the eccentricity, or axial ratio, of the particles ($\varepsilon < 1$ for a prolate spheroid; $\varepsilon > 1$ for an oblate spheroid; $\varepsilon = 1$ for a sphere).

The effects of varying core/shell size ratio can be seen in Figs. 1–3. The extinction efficiency is plotted vs. the equivalent-volume-sphere size parameter kr_{eq} for several values of core/shell ratio and eccentricities. From the data we cannot conclude whether coated spheroids scatter more or less than equal-volume spheres. Wang and Barber [12] showed some results for coated, oblate spheroids in fixed orientation that suggested a higher scattering power for non-spherical particles up to $kr_{eq} \sim 4$. Our data seem to show just the opposite: for small sizes, spherical particles scatter more than equivolume spheres. This apparent discrepancy can be explained in terms of the importance of relative core size in light scattering. Data from Figs. 1–3 show that spheres are better scatterers than equal-volume spheroids up to a certain size value kr_o; as the value of q increases, kr_o decreases and spheres are no longer better scatterers. Wang and Barber's particles have a fixed shell size parameter of about 0.03, so all but the smallest particles will have very large relative values of core (q close to 1). The region of very small particles is therefore characterized for moderate q values, for which we have found spherical particles to be better scatterers; this trend be also seen in Wang and Barber's data (Fig. 6c of [12]). It is noticeable that

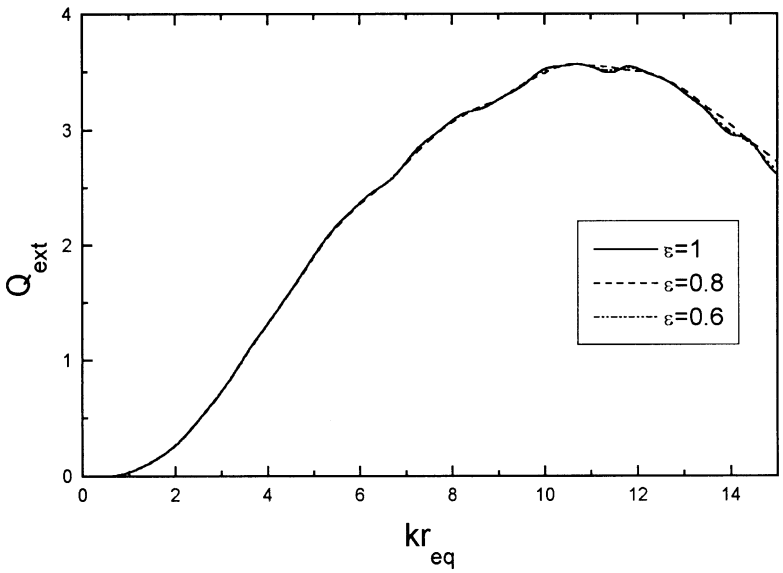

Fig. 1. Extinction efficiencies vs. equivalent-volume size parameter kr_{eq} for randomly oriented, coated spheroids with refractive indices (2.32, 1.2, 1) for core, shell and medium, respectively, and for a relative core size $q = 0.2$.

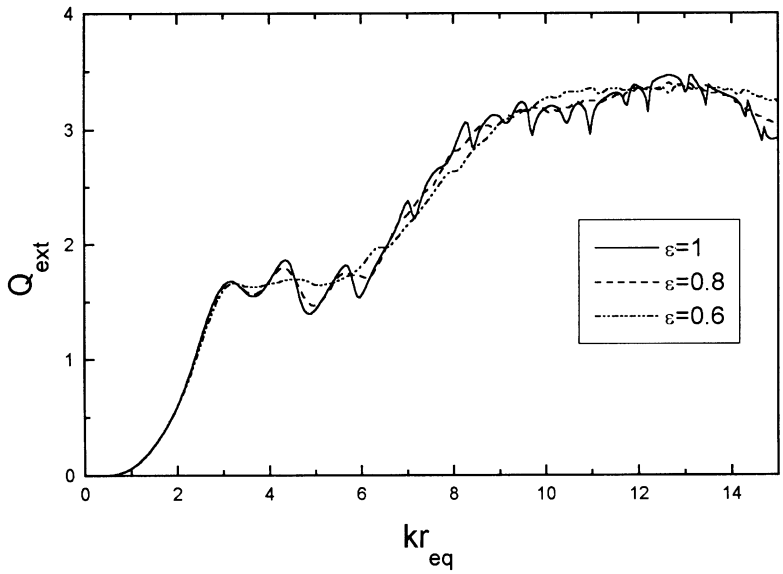

Fig. 2. Same as Fig. 1 for a relative core size $q = 0.4$.

spheres are also found to scatter more than equivolume spheroids for size parameters less than about 4 (see e.g. Ref. [25]).

We have plotted in Figs. 1–3 data only for prolate spheroids. That introduces an important question: do prolate and oblate coated spheroids scatter light differently? Figs. 4 and 5 plot the

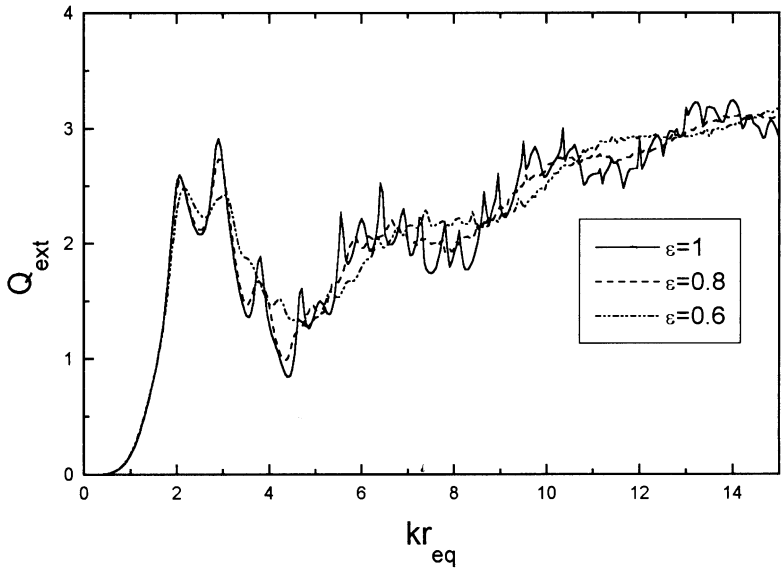

Fig. 3. Same as Fig. 1 for a relative core size $q = 0.6$.

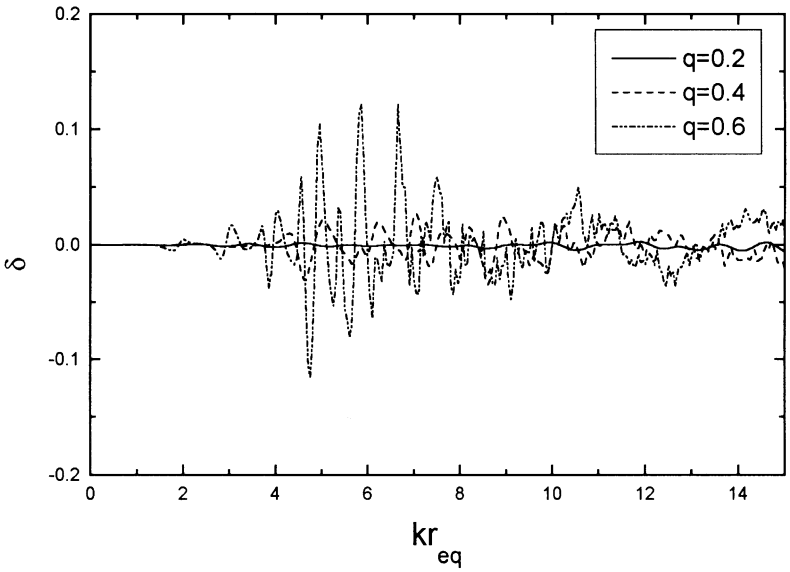

Fig. 4. Ratio $\delta = Q_{\mathrm{ext}}(\varepsilon^{-1})/Q_{\mathrm{ext}}(\varepsilon) - 1$, plotted against size parameter, between extinction efficiencies by oblate and prolate spheroids with the same volume and eccentricity $\varepsilon = 0.8$.

relative differences between extinction efficiencies for reciprocal particles, that is, prolate and oblate spheroids with the same volume and long-to-short axial ratio:

$$\delta = \frac{Q(\varepsilon^{-1})}{Q(\varepsilon)} - 1, \quad \varepsilon < 1. \tag{10}$$

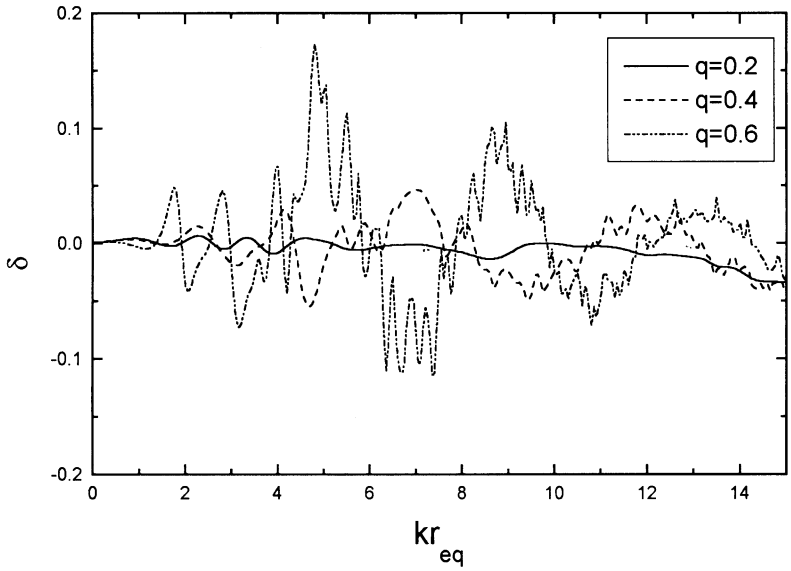

Fig. 5. Same as Fig. 4 for an eccentricity $\varepsilon = 0.6$.

It can be seen that prolate particles cannot be said to scatter more than oblate particles, nor vice versa. For the range of sizes ($kr_{eq} = 0$–15), relative core ratio ($q = 0.2$–0.6) and eccentricities ($\varepsilon = 0.8$–0.6) shown here, the extinction efficiencies for prolate and oblate particles do not differ by more than about 20%. It is to be noted that the greatest differences can be found at about $kr_{eq} \sim 4$–10. For small particles, light scattering depends on particle volume, not shape, so relative differences for equivolume particles tend to zero. On the opposite size range, cross section for very large particles are calculated as simply twice its cross section. Had we defined extinction efficiency as extinction cross section divided by the average projected area of particles in the ensemble, we should expect $Q_{ext} \to 2$, and therefore $\delta \to 0$, in the large particle limit. As we have used equivolume-sphere cross section, Q_{ext} will tend towards a different, shape-dependent limiting value. However, the differences between both surface parameter section (G in Eq. (9)) definitions are quite small; for G defined as the equivolume-sphere geometric cross sections, large-size-limit values of $\delta = 0.0006$ ($\varepsilon = 0.8$) and 0.0072 ($\varepsilon = 0.6$) are expected.

Fig. 4 shows such a trend ($\delta \to 2$) more clearly than Fig. 5, where a higher nonsphericity value is set. It can be seen that larger nonsphericity values increase the scattering differences between prolate and oblate particles. We can also see that, for a fixed eccentricity value, higher core (q) values also increase the differences. However, caution must be exercised in identifying this behavior as due to the nonsphericity of the system alone. It is known that Q_{ext} vs. size curves on spheres show an increasingly irregular ripple structure for higher, real refractive indices (Ref. [26], p. 106). Higher q values means that the particle contains a larger share of material with large refractive index, which can be seen as a Q_{ext}–kr curve where a ripple structure is more evident. This has been observed in coated spherical systems [22] and can also be appreciated in Figs. 1–3 for $\varepsilon = 1$. The effect of increasing nonsphericity is to smooth out the scattering efficiency curve; but the ripple

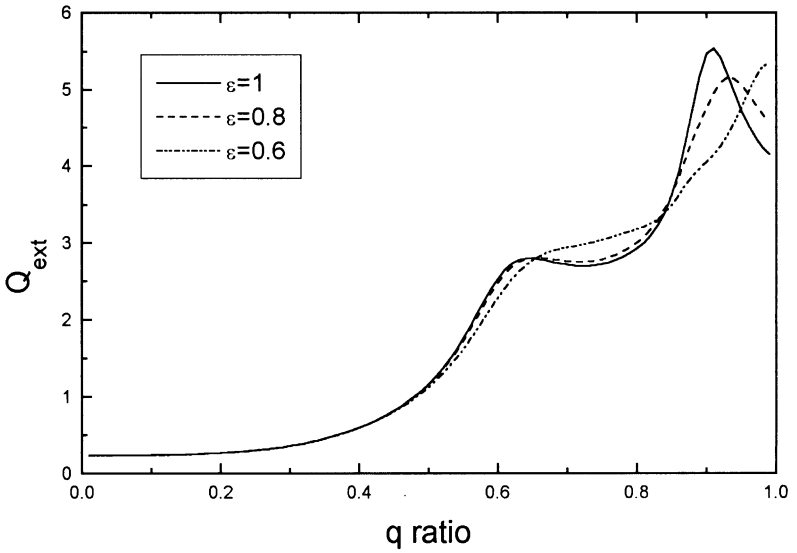

Fig. 6. Extinction efficiencies vs. relative core size q for randomly oriented, coated spheroids with refractive indices (2.32, 1.2, 1) for core, shell and medium, respectively, and for a dimensionless size parameter $kr_{eq} = 2$.

structure, while dimmed, is still present. This smoothing effect is carried out differently for oblate and prolate spheriods, as Figs. 5 and 6 show.

The effect of nonsphericity on randomly oriented coated spheroids can be better seen when the relative core parameter q is varied for a constant particle size. This is plotted for $kr_{eq} = 2$ (Fig. 6) and 5 (Fig. 7). Just as in the spherical case, it can be seen that scattering efficiencies are independent of the existence of a core up to a certain value of q. It is also found that particles with a larger size have its extinction efficiencies changed for smaller q. This leads us to conclude that coated spheroidal particles can be treated as homogeneous and the core effects disregarded only for small core values; on the other hand, large particles can generally not be regarded as homogeneous except for very small relative core sizes. In the opposite extreme, large core values, which means thin shells, show large extinction efficiency variations with small changes of shell thickness, specially for large size values for which $q - Q_{ext}$ show rapid variations. This has also been observed on coated spherical systems. Whether this is a common behavior for coated particle system, and to what extent does it depends on particle orientation (fixed or random) is an open subject and will require additional studies.

The differences of extinction efficiencies on the nonspherical character of the spheroids (prolate–oblate) are depicted in Figs. 8 and 9. We can see that small core values do not have any effect in the scattering properties of the particle. As the core grows larger, the differences become noticeable. We can see differences on the scattering behavior of equal-volume prolate and oblate spheroids, with no kind of particle being better scatterer than the other. However, it is remarkable how the smoothness of the δ–q curve for $kr_{eq} = 2$ (Fig. 8) vanishes for a larger size parameter ($kr_{eq} = 5$, Fig. 9). This implies that small changes in the core (or shell) size will lead to large differences in the scattering cross sections of thin-shelled oblate or prolate spheroids, thus suggesting that the

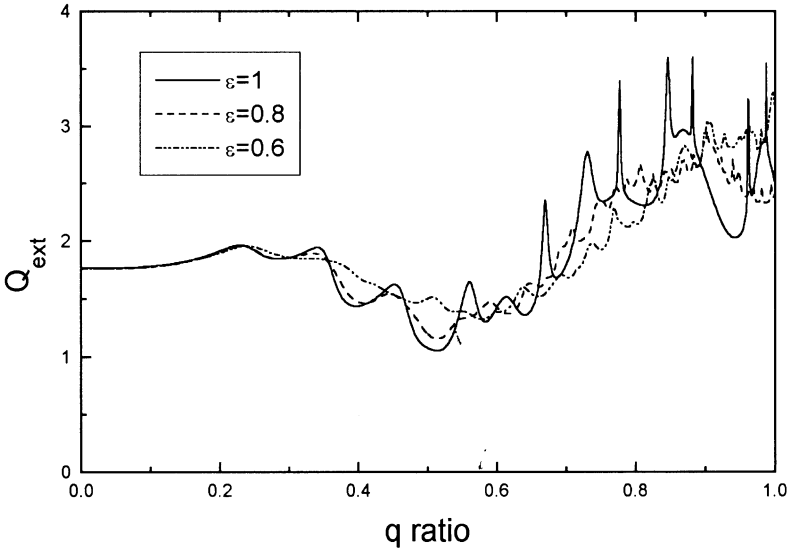

Fig. 7. Same as Fig. 6 for a size parameter $kr_{eq} = 5$.

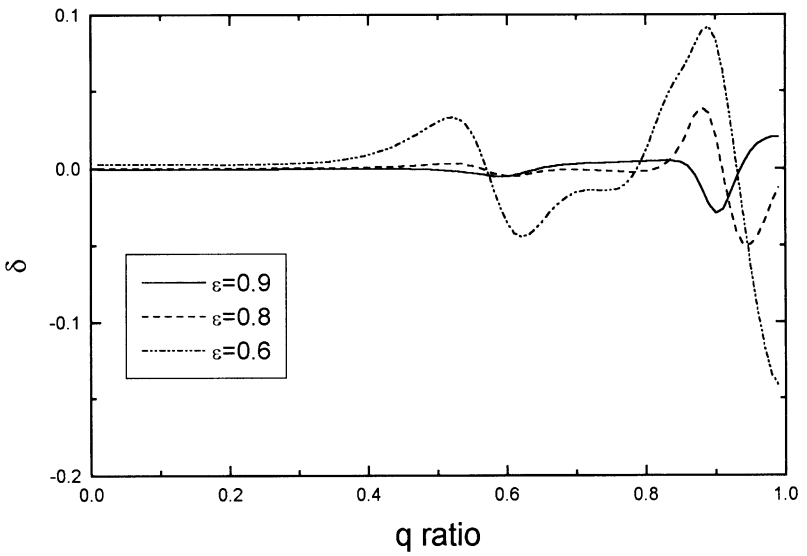

Fig. 8. Ratio $\delta = Q_{ext}(\varepsilon^{-1})/Q_{ext}(\varepsilon) - 1$, plotted against core/shell ratio, between extinction efficiencies by oblate and prolate spheroids with the same volume and size parameter $kr_{eq} = 2$.

Aden–Kerker simplification (coated spheres) can bring along uncertainties in the calculated cross section values for nonspherical particles, and that even the use of nonspherical particle theories in the case of small shell values can lead to incorrect results, depending on our assumption of particle shape.

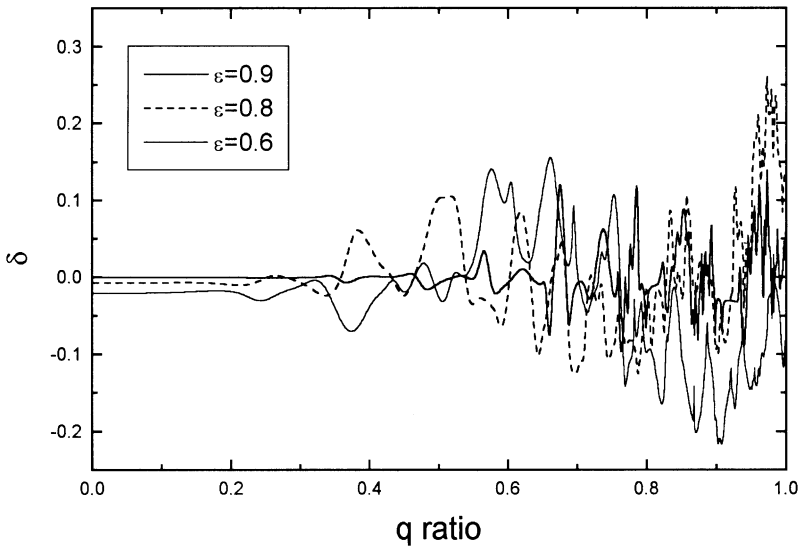

Fig. 9. Same as Fig. 8 for a size parameter $kr_{eq} = 5$.

On the other hand, the scattering differences between oblate and prolate spheroids are usually lower than the corresponding difference between nonspherical and spherical particles, specially in cases where a substantial part of the particle is made up of material with a high index of refraction. Thus, while it is necessary to accurately portray particle shape in thin shell cases, better results are achieved by assuming a nonspherical shape than by making a coated-sphere approximation. Nonspherical effects are known for other light scattering properties, such as linear polarization or backscattering; the same caution is due when dealing with cross sections.

4. Concluding remarks

We have presented the computed results for scattering efficiencies on coated spheroidal particle systems on random orientation using the T-matrix method. Adequate convergence procedures allow for an accurate calculation of light scattering properties. However, special care must be taken, as a T matrix for a coated spheroid is more ill-conditioned than its homogeneous counterpart. The reason lies in Eq. (6): the $\mathbf{AA}_2$ matrix elements depend on the product of two Hankel functions, which reach very high values when the matrix is large and/or the distance of the outer boundary to the center is small. So, in cases where particle is large or highly elongated, chances are higher that errors will arise.

We have found the Peterson–Ström [9] application of EBCM theory to yield accurate results on scattering and extinction cross sections for a certain size (0–15), core ratio (0–0.8) and eccentricity (0.5–2) range. It would be desirable to be able to apply this method to other size and shape ranges. In some cases (data not show), convergence was not achieved for our accuracy requirements; in others, CPU consumption was excessively large.

Whether calculations on coated spheroids can be made as accurately as in the homogeneous case is still an open question. We have found, for instance, that the use of extended precision or a higher number of Gauss quadrature points have only marginal benefits in terms of accuracy. Our efforts are currently focused in trying to overcome this limitation without having to resort to other, more complex and time-consuming T-matrix variants like the iterative extended boundary condition method (IEBCM) [27].

We have directed our efforts to building T-matrix implementations that can be run on multiple platform types. To that goal, a Fortran-77 code has been built that can be compiled and run either on Unix-based platforms or on PC machines. The loss of speed can be compensated by the advantages in flexibility, portability and ease of use. The calculations showed in the present paper represent calculations for a total of 11,100 individual particles in random orientation, with a combined CPU usage of 120 h on Pentium computers (133–200 Mhz, 16–32 M bit RAM).

Finally, the results we have shown can be used in light scattering sizing techniques. In turbidity experiments, extinction cross sections are measured for a number of wavelengths (and, consequently, different size parameters). A comparison with theoretical curves such as those depicted in Figs. 1–3 can yield information on eccentricity and core size by finding the theoretical curve — calculated for a given (ε, q) — that best approaches experimental data. Actual applications would require careful attention to effects such as polydispersity or wavelength-dependent refractive index.

Acknowledgements

We are grateful to Dr. K. Aydin (Penn State University, Pennsylvania, USA) for valuable discussions. Financial support for this research was provided by DGICYT, Spain (Project · MAT98-0940).

References

[1] Waterman PC. Phys Rev D 1971;3:825.
[2] Barber PW. IEEE MTT 1977;25:373.
[3] Scheiner JB, Peden IC. IEEE AP 1988;36:1317.
[4] Tsang LT, Kong JA, Shin RT. Radio Sci 1984;19:629.
[5] Mishchenko MI. J Opt Soc Am A 1991;8:871.
[6] Mishchenko MI. Appl Opt 1993;32:4652.
[7] Aden AL, Kerker M. J Appl Phys 1951;22:1242.
[8] Bohren CB, Huffman DR. Absorption and scattering of light by small particles. New York: Wiley, 1983.
[9] Peterson B, Ström S. Phys Rev D 1974;10:2670.
[10] Ström S. Phys Rev D 1974;10:2685.
[11] Kristensson G. J Appl Phys 1980;51:3486.
[12] Wang D-S, Barber PW. Appl Opt 1979;18:1190.
[13] Wang D-S, Chen HCH, Barber PW, Wyatt PJ. Appl Opt 1979;18:2672.
[14] Asano S, Yamamoto G. Appl Opt 1975;14:29.
[15] Al-Rizzo HM, Tranquilla JM. J Comp Phys 1995;119:342.
[16] Al-Rizzo HM, Tranquilla JM. J Comp Phys 1995;119:356.
[17] Wiscombe WJ, Mugnai A. Appl Opt 1986;25:1235.

[18] Stratton JA. Electromagnetic theory. New York: McGraw-Hill, 1941.
[19] Wiscombe WJ. Appl Opt 1980;19:1505.
[20] Mackowski DW, Altenkirch RA, Menguc MP. Appl Opt 1990;29:1551.
[21] Kerker M, Scheiner P, Cooke DD, Kratohvil JP. J Coll Int Sci 1979;156:56.
[22] Quirantes A, Delgado AV. J Phys D 1997;30:2123.
[23] Van de Hulst HC. Light scattering by small particles. New York: Dover Publications, 1957.
[24] Kuik F. Single scattering of light by ensembles of particles with various shapes. Ph.D. thesis. University of Amsterdam, 1992.
[25] Mishchenko MI, Travis LD. Appl Opt 1994;33:7206.
[26] Kerker M. The scattering of light and other electromagnetic radiation. San Diego: Academic Press, 1969.
[27] Iskander MF, Lakhtakia A, Durney CH. Proc IEEE 1982;70:1361.